Molecular orbital studies (hardness, chemical potential, electrophilicity, and first electron excitation), vibrational investigation and theoretical NBO analysis of 2-hydroxy-5-bro...

ARTICLE *in* JOURNAL OF MOLECULAR STRUCTURE · JANUARY 2013

Impact Factor: 1.6 · DOI: 10.1016/j.molstruc.2012.09.047

3 AUTHORS, INCLUDING:

Dr Vadivelu Balachandran
A.A.Government Arts College Musiri
155 PUBLICATIONS **672** CITATIONS
SEE PROFILE

T. Karthick
University of Lucknow
30 PUBLICATIONS **101** CITATIONS
SEE PROFILE

Journal of Molecular Structure 1031 (2013) 221–233

Contents lists available at SciVerse ScienceDirect

Journal of Molecular Structure

journal homepage: www.elsevier.com/locate/molstruc

Molecular orbital studies (hardness, chemical potential, electrophilicity, and first electron excitation), vibrational investigation and theoretical NBO analysis of 2-hydroxy-5-bromobenzaldehyde by density functional method

A. Nataraj [a], V. Balachandran [b,*], T. Karthick [c]

[a] PG and Research Department of Physics, Thanthai Hans Roever College, Perambalur 621 212, India
[b] PG and Research Department of Physics, A.A. Govt. Arts College, Musiri, Tiruchirapalli 621 211, India
[c] Department of Physics, Vivekanandha College for Women, Tiruchengode 637 205, India

HIGHLIGHTS

- Vibrational spectroscopy of HBB by means of quantum chemical calculations.
- The FT-IR, FT-Raman spectral investigation of HBB has been performed using DFT.
- The redistribution of electron density has been discussed.
- The molecular orbital studies and excitation energies were calculated.
- The chemical reactivity of the molecule was explained.

ARTICLE INFO

Article history:
Received 8 June 2012
Received in revised form 22 August 2012
Accepted 17 September 2012
Available online 13 October 2012

Keywords:
2-Hydroxy-5-bromobenzaldehyde
Orbital studies
NBO analysis
Electrostatic potential
Hyperpolarizability

ABSTRACT

In this work, the vibrational spectral analysis was carried out using Raman and infrared spectroscopy in the range 4000–400 cm^{-1} and 3500–100 cm^{-1}, respectively, for the 2-hydroxy-5-bromobenzaldehyde (HBB). The experimental spectra were recorded in the solid phase. The fundamental vibrational frequencies and intensity of vibrational bands were evaluated using density functional theory (DFT) with the standard B3LYP/6-311G++(d,p) method and basis set. Normal co-ordinate calculations were performed with the DFT force field corrected by a recommended set of scaling factors yielding fairly good agreement between observed and calculated frequencies. Simulation of infrared and Raman spectra utilizing the results of these calculations led to excellent overall agreement with the observed spectral patterns. The complete assignments were performed on the basis of the potential energy distribution (PED) of the vibrational modes, calculated with scaled quantum mechanics (SQM) method. The optimized geometric parameters (bond lengths and bond angles) were compared with experimental values of related compound. The stability of the molecule arising from hyper conjugative interactions and the charge delocalization has been analyzed using natural bond orbital (NBO) analysis. The directly calculated ionization potential (IP), electron affinity (EA), electronegativity (χ), electrophilicity index (ω), hardness (η), chemical potential (μ), and first electron excitation (τ) are all correlated with the HOMO and LUMO energies with their molecular properties. These show that charge transfer occurs within the molecule. Furthermore, molecular electrostatic potential maps (MESP) of the molecule have been calculated.

1. Introduction

Benzaldehyde derivatives such as p-hydroxy-benzaldehyde, p-chlorobenzaldehyde, anisaldehyde are used in the synthesis of biologically active polymers, for example, in Chitosan derivatives, which are known for application in cosmetics, textiles, as biomaterials and for anti-microbial activity [1]. Benzaldehyde derivatives treated with base to form a substituted chalcone, which has been found to have anti-cancer properties [2]. Several workers have investigated vibrational spectroscopic properties, such as the mutual influence of different types of substituents such as halogens, methyl, methoxy and hydroxyl on benzaldehyde the interactions between the ring and substituents, by joint experimental and/or theoretical methods [3–12]. Spectroscopy of aromatic molecular systems containing hydroxyl and aldehydic groups such as benzaldehyde, phenol and salicylaldehyde as a function of substitution type and pattern has been of interest as they are chemically and

* Corresponding author. Tel.: +91 431 2591338; fax: +91 4326 262630.
E-mail address: brsbala66@gmail.com (V. Balachandran).

0022-2860/$ - see front matter © 2012 Elsevier B.V. All rights reserved.
http://dx.doi.org/10.1016/j.molstruc.2012.09.047

biologically interesting systems [3]. Investigation of vibrational spectra of benzaldehyde and its mono-substituted derivatives were reported by Green and Harrison [4]. Recently, Lampert et al. have studied *ab initio* and DFT structures and normal modes of phenol, benzaldehyde and salicylaldehyde [5]. Normal coordinate analysis for *o*-, *m*-, *p*-trifluoromethyl benzaldehydes have been reported by Yadav and Singh [6]. Extensive study on *ortho* substituted derivatives with special references to the type of hydrogen bonding is due to Pinchas [7]. Infrared and Raman spectral studies and evaluation of force fields for isomeric methoxybenzaldehyde and dihydroxybenzaldehyde have been reported by Singh [8]. Spectroscopic studies revealing hydrogen bonding in substituted benzaldehydes in liquid phase giving insight on dimmeric species have been reported [9]. The conformation stability, molecular vibrations, HOMO–LUMO energy, Mulliken atomic charges and intra-molecular charge transfer on tri-substituted benzaldehyde were reported in our earlier work [10]. Study on the *cis* and *trans* conformers of *ortho*- and *meta*-chlorobenzaldehydes have been done by Bednarek et al. [11]. A thorough investigation of the molecular structures of salicylaldehyde and the effect of intramolecular hydrogen bonding on the geometry of its possible conformers has been carried out by Chung et al. [12]. Ribeiro-Claro et al. have investigated C—H···O bonding assisted interactions in 2-methoxybenzaldehyde and 4-methoxybenzaldehyde from X-ray, vibrational and *ab initio* studies [9,13].

In the present work, harmonic-vibrational frequencies calculated for *cis* and *transcis-A* conformers of 2-hydroxy-5-bromobenzaldehyde using B3LYP/6-311++G(d,p) method. The calculated spectra of these two conformers are compared to that of experimentally observed FT-IR and FT-Raman spectra. The redistribution of electron density (ED) in various bonding and antibonding orbitals and $E(2)$ energies has been calculated by natural bond orbital (NBO) analysis by DFT method to give clear evidence of stabilization originating from the hyper conjugation of various intramolecular interactions. The HOMO and LUMO analysis have been used to elucidate information regarding ionization potential (IP), electron affinity (EA), electronegativity (χ), electrophilicity index (ω), hardness (η), chemical potential (μ), and first electron excitation (τ) are all correlated. These are confirming the charge transfer within the molecule and also molecular electrostatic potential (MESP) contour map show the various electrophilic region of the title molecule. However, molecular hyperpolarizability is also calculated by DFT method. Finally, the correlations between thermodynamic properties with various temperatures are reported.

2. Experimental details

The compound 2-hydroxy-5-bromobenzaldehyde in the solid form was purchased from the Sigma–Aldrich Chemical Company (US), with a stated purity of greater than 98% and it was used as such without further purification. The FT-Raman spectrum of title molecule has been recorded using the 1064 nm line of a Nd:YAG laser as excitation wavelength in the region 100–3500 cm^{-1} on a BRUCKER model IFS 66 V spectrometer. The reported wavenumbers are expected to the accurate within ±1 cm^{-1}. The FT-IR spectrum of this compound was recorded in the region 400–4000 cm^{-1} on IFS 66 V spectrometer equipped with an MCT detector using KBr beam splitter and globar source. The data were recorded in the co-addition of 200 scans at ±1 cm^{-1} resolution with 250 mW of power at the sample in both the techniques.

3. Prediction of Raman intensity

The Raman activities (S_{Ra}) calculated with the Gaussian 09 program [14] were converted to relative Raman intensities (I_{Ra}) using the following relationship derived from the intensity theory of Raman scattering [15–17].

$$I_{Ra} = \frac{f(v_0 - v_i)^4 S_{Ra}}{v_i[1 - \exp(-hcv_i/kT)]}$$

where v_0 is the laser exciting frequency in cm^{-1} (in this work, we have used the excitation wavenumber v_0 = 9398.5 cm^{-1}, which corresponds to the wavelength of 1064 nm of a Nd:YAG laser), v_i is the vibrational wavenumber of the ith normal mode (in cm^{-1}) and S_{Ra} is the Raman scattering activity of the normal mode v_i, f (is the constant equal to 10^{-12}) is the suitably chosen common normalization factor for all peak intensities. h, k, c, and T are Planck constant, Boltzmann constant, speed of light, and temperature in Kelvin, respectively.

4. Computational details

The entire calculation was performed at DFT/B3LYP/6-311++G(d,p) large basis set on personal computer using Gaussian 09W [14] program package, invoking gradient geometry optimization [18]. The global minimum energy conformer and *transcis-A* (the energy nearer to the minimum energy conformer) were used in the vibrational wavenumber calculation at the DFT/B3LYP/6-311++G(d,p) level to characterize all stationary points as minima. As a result, the unscaled calculated wavenumbers, reduced masses, force constants, infrared intensities, Raman activities, and depolarization ratios are obtained. In order to fit the theoretical wavenumbers to the experimental, the scaling factors have been introduced by using a least square optimization method. The calculated vibrational wavenumbers are scaled as 0.9547 for wavenumbers above 1700 cm^{-1} and below 1700 cm^{-1} scaled as 0.9899 for B3LYP [19]. After scaled with the scaling factor, the deviation from experiments is less than 15 cm^{-1} with a few exceptions. In addition to that we have used scaled value for *transcis-A* conformer are 0.9964, 0.9187 for wavenumber less than and greater than of 1700 cm^{-1}, respectively. For vibrational assignments, symmetry coordinates in terms of potential energy distribution (PED) have been computed from a normal coordinate analysis in the MOLVIB program [20]. The natural bonding orbital (NBO) calculation were performed using NBO3.1 program as implemented in Gaussian 09W [14] package at DFT/B3LYP/6-311++G(d,p) level in order to understand various second order interactions between the another subsystem, which is a measure of the intramolecular delocalization or hyper-conjugation.

5. Result and discussion

5.1. Conformational analysis

The conformation of HBB is related to different rotamers, we have determined four conformers for title molecule by defining orientation of the —CHO and —OH groups with respect to the Br atom. The total energies obtained from the four conformers are presented in Table 1. In labeling the conformers (*cis*, *transcis-A*, *trans*, *and transcis-B*), we call the conformer *trancis* when one group, say, —CHO, is *trans* and other group, —OH, is *cis* to Br atom conversely. Thus, the molecular structure of the most stable conformer with numbering is shown in Fig. 1a and/or Fig. 2. All the conformers have been optimized utilizing the tight convergence criteria yielding planar structures with C_s symmetry; they are shown in Fig. 1. From the four conformational structures, *cis* is found to be the most stable with energy of −7861926.29 kJ/mol. the other three conformers of energy differences are increasing in the order of *transcis-A*, *trans* and *transcis-B*. In Table 1, the energy differences between the conformers with respect to the most

Table 1
Total energy of different conformations are 2-hydroxy-5-bromobenzaldehyde calculated at the DFT (B3LYP)/6-311++G(d,p) level of theory.

Conformers	Total energies (Hartrees) 6-311++G(d,p)	Total energies (kJ/mol) 6-311++G(d,p)	Energy different ΔE with respect to cis[a] (Hartrees)	Energy different ΔE with respect to cis[a] (kJ/mol)
cis[a]	−2994.44894	−7861926.29	0.00	0.00
transcis-A	−2994.43652	−7861893.682	0.01242	32.608
trans	−2994.40490	−7861810.663	0.04404	115.627
transcis-B	−2994.39640	−7861788.347	0.05254	137.943

[a] Global minimum energy (stable conformer).

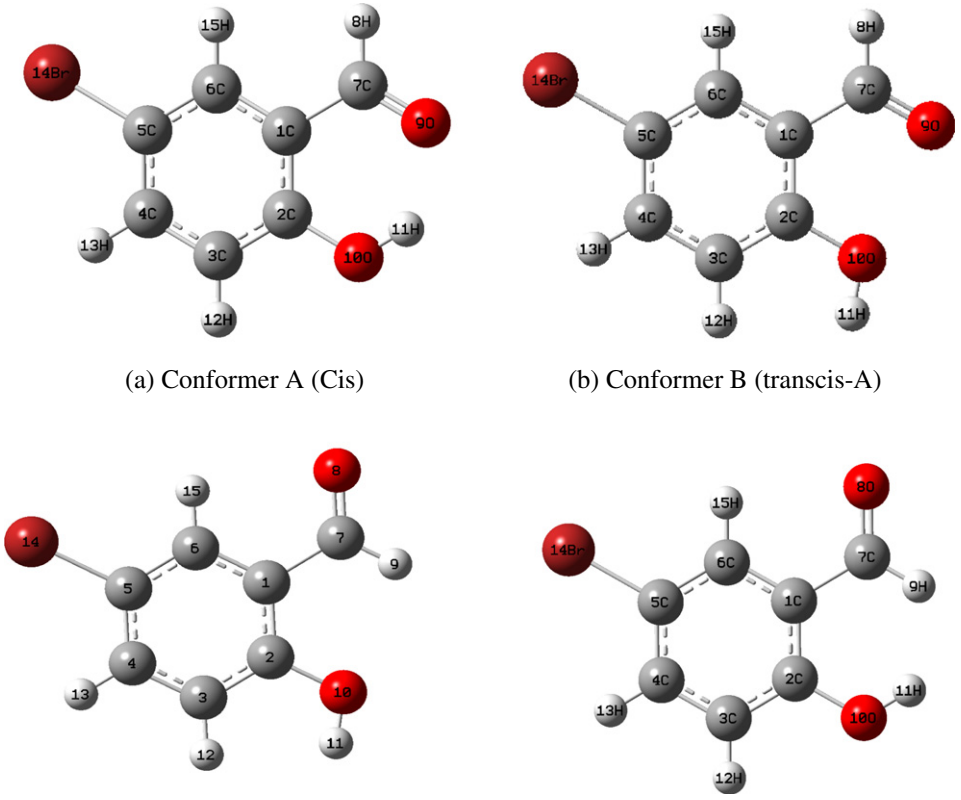

Fig. 1. (a–d) Possible conformational structure for 2-hydroxy-5-bromobenzaldehyde.

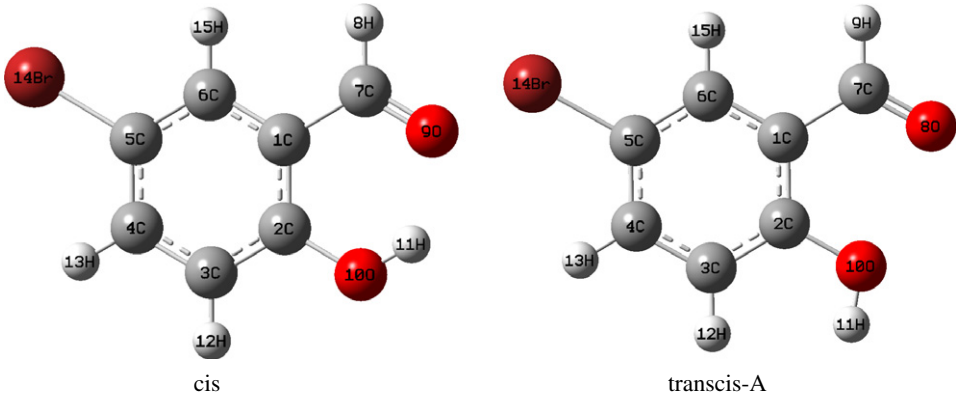

Fig. 2. The theoretical geometric structure and atoms numbering of cis and *transcis-A* conformers for 2-hydroxy-5-bromobenzaldehyde.

Table 2
Optimized geometrical parameters of 2-hydroxy-5-bromobenzaldehyde at B3LYP/6-311++G(d,p) level.

Bond length (Å)	[a]Experimental value (Å)	Calculated value (Å)	Bond angle	Experimental value	Calculated value	Dihedral angle	Value
C1—C2	1.404	1.4057	C2—C1—C6	119.9	119.2945	C6—C1—C2—O10	180.0
C1—C6	1.399	1.4017	C2—C1—C7	119.7	121.4402	C7—C1—C2—C3	180.0
C1—C7	1.482	1.4846	C6—C1—C7	120.9	119.2653	C2—C1—C6—H15	180.0
C2—C3	1.392	1.3971	C1—C2—C3	121.8	119.8648	C7—C1—C6—C5	180.0
C2—O10	1.362[b]	1.3632	C1—C2—O10	121.2	118.1351	C2—C1—C7—H8	180.0
C3—C4	1.400	1.3895	C3—C2—O10	121.2	122.0001	C6—C1—C7=O9	180.0
C3—H12	1.094	1.0858	C2—C3—C4	121.0	120.3388	C1—C2—C3—H12	180.0
C4—C5	1.394	1.3957	C2—C3—H12	121.0	119.99	C2—C3—C4—O10	180.0
C4—H13	1.094	1.0824	C4—C3—H12	119.5	119.6712	O10—C2—C3—H12	0.00
C5—C6	1.398	1.3836	C3—C4—C5	119.0	119.7107	C1—C2—O10—H11	180.0
C5—Br14	1.734	1.9162	C3—C4—H13	121.0	119.9533	C3—C2—O10—H11	0.00
C6—H15	1.094	1.0828	C5—C4—H13	119.5	120.336	C2—C3—C4—C5	0.00
C7—H8	1.117	1.2129	C4—C5—C6	121.2	120.5297	C2—C3—C4—H13	180.0
C7=O9	1.216	1.1029	C4—C5—Br14	–	119.3567	H12—C3—C4—C5	180.0
O10—H11	0.985[b]	0.9631	C6—C5—Br14	119.5	120.113	H12—C3—C4—H13	0.00
			C1—C6—C5	118.2	120.2615	C3—C4—C5—Br14	180.0
			C1—C6—H15	118.2	117.9699	H13—C4—C5—C6	180.0
			C5—C6—H15	119.5	121.7686	C4—C5—C6—H15	180.0
			C1—C7—H8	125.5	123.4841	Br14—C5—C6—C1	180.0
			C1—C7=O9	116.0	115.6301		
			H8—C7=O9	118.5	120.8858		
			C2—O10—H11	106.4	110.1851		

Notes: Bond lengths are in Å, bond angles and dihedrals are in degrees.
[a] X-ray data taken from Ref [19].
[b] Ref [3].

stable conformer *cis* are given. This may be explained as follows: the bromine at the 5th position (*meta*) in HBB shows torsional strain (a potential barrier) due to the repulsion experienced by the bonding electrons of aldehydic oxygen and that of bromine when they get too close. When the 5th position (*meta*) of bromine in HBB, the torsional strain is considerably reduced thereby is making the —CHO group free to rotate and this result in two conformers with nearly equal energies. It is also to be noted that the other energy differences of the conformers *trans*, and *transcis-B* with respect to the *cis* are rather close to each other suggesting that the two substituent's, bromine and —OH group.

5.2. Molecular geometry

The optimized geometries of the most stable conformer Fig. 1a are performed by DFT/B3LYP level with 6-311G++(d,p) basis set. The optimized bond lengths, bond angles and dihedral angles of title compound are listed in Table 2. In this present work, geometry optimization parameters for 2-hydroxy-5-bromobenzaldehyde have been employed without symmetry constrain. Since the crystal structure of the title compound is not available till now, the optimized structure can be compared with other similar systems and with the available X-ray data, from which the crystal structure has been solved [5,21].

From the theoretical values, we can find that most of the optimized bond lengths are slightly larger than the experimental values, due to that the theoretical calculations belong to isolated molecule in gaseous phase and the experimental results belong to molecule in solid state. In this case the Br14 to ring C5 distance is 1.9162 Å relatively 0.1822 Å longer than the X-ray diffraction (XRD)[21], due to the electron – withdrawing effects depending on the presence of the carbonyl groups linked to these bonds. The C—C aromatic bond distances fall in the range from 1.3836 to 1.4057 Å for the B3LYP/6-311G++(d,p) method, which are in good agreement with those in molecular structure of 4-chlorobenzaldehyde (1.392–1.404 Å) [21]. The optimized C_{ring}—$C7_{aldehyde}$ bond length is 1.4846 Å which is slightly longer than that in 4-chlorobenzaldehyde (1.482 Å) and the results show difference in ~0.0026 Å. In aldehyde group C=O bond length 1.2129 Å and C—H bond length 1.212 Å are compared with the X-rd data the results show C=O is slightly shorter (~0.1131 Å) and C—H is slightly longer (~0.0959 Å).

Dipole moment reflects the molecular charge distribution and is given as a vector in three dimensions. Therefore, it can be used as descriptor to depict the charge movement across the molecule. Direction of the dipole moment vector in a molecule depends on the centers of positive and negative charges. Dipole moments are strictly determined for neutral molecule. For charged system, its value depends on the choice of origin and molecular orientation.

Mulliken atomic charge calculation has an important role in the molecular system because it is used to interpret the atomic charges effect, dipole moment, molecular polarizability, electronic structure and more a lot of properties of molecular system. The calculated Mulliken's charge values are listed in Table 3. Significant change in the atomic charges of carbon atoms C1, C2, and C5 were found in the *cis* conformer arises upon the electronic effects by the substituents such as aldehyde, hydroxyl and bromine groups attached with them. Considering the charges of HBB, the atoms C1 having more positive (2.0549 eV), and C5 having less positive (0.3400 eV) charge calculated in B3LYP/6-311++G(d,p) method indicates the high electron withdrawing nature, as it is linked between the neighboring aldehyde and bromine through the single bond, respectively. Likewise, high negative values were observed in bromine (−0.1732 eV) and O10 (−0.2100 eV) in B3LYP/6-311++G(d,p) method indicates the high electron donating nature. The results may suggest the presence of intra-molecular interactions in the solid forms.

5.3. NBO analysis

Natural bond analysis gives the accurate possible natural Lewis structure picture of φ because all orbital mathematically chosen to include the highest possible percentage of the electron density. Interaction between both filled and virtual orbital spaces information correctly explained by the NBO analysis, it could enhance the analysis of intra- and intermolecular interactions. The second order Fock matrix was carried out to evaluate donor (i) acceptor (j) i.e. donor level bonds to acceptor level bonds interaction in the NBO

Table 3
Calculated thermodynamic parameters and Mulliken atomic charges of cis and *transcis-A* conformers for 2-hydroxy-5-bromobenzaldehyde employing DFT/B3LYP/6-311G++(d,p).

Thermodynamic parameters (298 K)	B3LYP/6-311G++(d,p).		Atoms	Atomic charges (Mulliken)	
	cis	*transcis-A*		*cis*	*transcis-A*
SCF energies (a.u.)	−622.077821423		C1	2.0549	0.7995
Total energy (thermal), E_{total} (Kcal mol^{-1})	70.356	69.130	C2	−2.2621	−0.2270
Heat capacity at constant volume, Cv (cal mol^{-1} K)	33.280	32.327	C3	0.5363	−0.2289
Entropy, S (cal mol^{-1} K)	95.951	92.850	C4	−0.3509	0.1420
Vibrational energies, E_{vib} (kJ mol^{-1})	68.578	67.352	C5	0.3400	0.00916
Zero point vibrational energy (J mol^{-1})	270366.1	266702.9	C6	−0.7711	−0.8386
Rotational constants (GHz)			C7	0.0203	−0.0650
A	1.750	2.475	H8	0.1773	−0.2150
B	0.509	0.4384	O9	−0.2434	0.1520
C	0.395	0.3724	O10	−0.2100	−0.1879
Dipole moment (Debye)			H11	0.2664	0.2555
μ_x	2.5169	−2.0806	H12	0.1484	0.1359
μ_y	− 4.6514	2.1967	H13	0.2273	0.2244
μ_z	0.00	0.2856	Br14	−0.1732	−0.1779
μ_{total}	5.2887	3.0391	H15	0.2398	0.2217

Table 4
Second-order perturbation theory analysis of Fock matrix in NBO basis corresponding to the intramolecular bonds of 2-hydroxy-5-bromobenzaldehyde.

Donor (*i*)	ED (*i*) (e)	Acceptor (*j*)	ED (*j*) (e)	[a]*E*(2) (kJ mol^{-1})	[b]*E*(*j*)−*E*(*i*) (a.u.)	[c]*F*(*i*,*j*) (a.u.)
σC1−C2	1.97443	σ*C1−C7	0.0603	0.97	1.10	0.029
		σ*C7−O8	0.00203	0.64	1.26	0.025
		σ*O10−H11	0.00559	1.05	1.13	0.031
σC2−O10	1.99345	σ*C1−C6	0.01981	1.68	1.42	0.044
		σ*C3−C4	0.01637	1.34	1.41	0.039
σC5−Br14	1.9852	σ*C1−C6	0.01981	2.62	1.21	0.05
		σ*C3−C4	0.01637	2.76	1.21	0.051
πC7−O9	1.99642	π*(C1−C2)	0.02659	1.03	1.55	0.036
σC7−H8	1.98968	σ*C1−C6	0.01981	2.74	1.11	0.049
σO10−H11	1.98936	σ*C1−C2	0.02659	3.56	1.31	0.061
πO9 (LP1)	1.98043	π*(C1−C7)	0.05585	1.46	1.09	0.036
		π*(O10−H11)	0.02773	2.77	1.20	0.052
σO9 (LP2)	1.89361	σ*(C7−H8)	0.04178	16.29	0.70	0.097
πO10 (LP2)	1.85472	π*(C2−C3)	0.35564	24.82	0.32	0.084
πBr14 (LP1)	1.99347	π*(C4−C5)	0.02585	1.62	1.54	0.045
		π*(C5−C6)	0.02554	1.62	1.54	0.045
σBr14 (LP2)	1.97480	σ*(C4−C5)	0.40196	3.41	0.85	0.048

[a] *E*(2) means energy of hyperconjugative interactions.
[b] Energy difference between donor and acceptor *i* and *j* NBO orbitals.
[c] *F*(*i*,*j*) is the Fock matrix element between *i* and *j* NBO orbitals.

analysis [22]. The result of interaction is a loss of occupancy from the concentrations of electron NBO of the idealized Lewis structure into an empty non-Lewise orbital. For each donor (*i*) and acceptor (*j*), the stabilization energy *E*(2) associates with the delocalization $i \rightarrow j$ is estimated as.

$$E_2 = \Delta E_{ij} = q_i \frac{F(i,j)^2}{\varepsilon_j - \varepsilon_i}$$

where q_i is the donor orbital occupancy, are ε_j and ε_i diagonal elements and *F*(*i*,*j*) is the off diagonal NBO Fock matrix element. Natural bond orbital analysis is used for investigating charge transfer or conjugative interaction in the molecular system. Some electron donor orbital, acceptor orbital and the interacting stabilization energy resulted from the second-order micro-disturbance theory are reported [23,24]. The larger *E*(2), value the more intensive is the interaction between electron donors and acceptor, i.e. the more donation tendency from electron donors to electron acceptors and the greater the extent of conjugation of the whole system [25]. Delocalization of electron density between occupied Lewis-type (bond or lone pair) NBO orbitals and formally unoccupied (antibond or Rydgberg) non-Lewis NBO orbitals correspond to a stabilization donor–acceptor interaction. NBO analysis has been performed on the *cis* conformer of HBB molecule at the DFT/B3LYP/6-311++G(d,p) level in order to elucidate the intramolecular, rehybridization and delocalization of electron density within the molecule.

The intramolecular interaction is formed by the orbital overlap between σ (C5—Br14) and σ*(C3—C4), σ*(C1—C6) bond orbital, which results intramolecular charge transfer causing stabilization of the system. The most important interactions in the title molecule having lone pair O10(2) with that of antibonding C2—C3 and the lone pair O9(2) with that of antibonding C7—H8, results the stabilization of 24.82 kJ/mol and 16.29 kJ/mol, respectively, which donates larger delocalization. The maximum energy transfer occurs from LPO9(2) and LPO(10) to C2—C3 and C7—H8 as shown in Table 4. The ED in O9(2) and O10(2) lone pairs are moderates increased the electron density of σ*(C7—H8) and π*(C2—C3) are of 0.04178 e and 0.35564 e, respectively, which yields to weakening the bond and its elongation (0.059 and 0.0051 Å) from the experimental value of the title molecule.

5.4. Vibrational analysis

The title molecule consists of 15 atoms, and so they have 39 normal vibrational modes. On the assumption of C_s symmetry, the number of vibrational modes of the 39 fundamental vibrations

is divided into $27A' + 12A''$. The vibrations of the A' species are in-plane modes and those of the A'' species are out-of-plane modes. All fundamental vibrations are active in both IR absorption and Raman scattering. The calculated harmonic wavenumbers are usually higher than the corresponding experimental quantities because of the combination of electron correlation effects and basis set deficiencies. Nevertheless, after applying a uniform scaling factor, the theoretical calculation reproduces the experimental data well. The experimental FT-IR and FT-Raman and theoretical spectra of title molecule are shown in Figs. 3 and 4. The observed and calculated wavenumbers for *cis* and *transcis-A* conformers along with their relative intensities and probable assignments with PEDs are summarized in Table 5. The observed slight disagreement between theory and experimental could be noted that the calculations were made for a free molecule in vacuum, while experiments were performed for solid samples. Furthermore, the anharmonicity is neglected in the real system for the calculated vibrations.

5.4.1. Hydroxyl and CO vibrations

The O—H group gives rise to three vibrations (stretching, in-plane bending and out-of-plane bending vibrations). The O—H group vibrations are likely to be the most sensitive to the environment, so they show pronounced shifts in the spectra of the hydrogen bonded species. The hydroxyl stretching vibrations are generally [26–28] observed in the region around 3500 cm^{-1}. In the present case, a medium–strong broad absorption at 3366 cm^{-1} (IR) and 3363 cm^{-1} (Raman) are assigned to O—H stretching vibration. The stretching vibrational wavenumber of free O—H is practically unchanged, while that of the bound O—H is red shifted. The red shift of the O—H stretching wavenumber is due to the formation of strong O—H···O hydrogen bonds by hyperconjucation between aldehydic oxygen lone electron pairs and σ^{*-} O—H antibonding orbitals. This is due to the increase of electron density occurring at σ^{*}C═O and the antibonding orbitals σ^{*}O—H. consequently, these bonds become weaker and are elongated, and the respective stretching vibrational wavenumbers are red shifted [28]. Similarly in our case also the theoretical calculation of *cis* conformer predict the anharmonic wavenumber at 3339 cm^{-1} by B3LYP method is assigned to O—H stretching vibration, this wavenumber show negative deviation about 27 cm^{-1}, this may be due to presence of hydrogen bonding between aldehyde and hydroxyl groups. The in-plane bending vibration of O—H in the region 1650–1000 cm^{-1}, taken as the second criterion, is expected to increase in its wavenumber and is known as couple

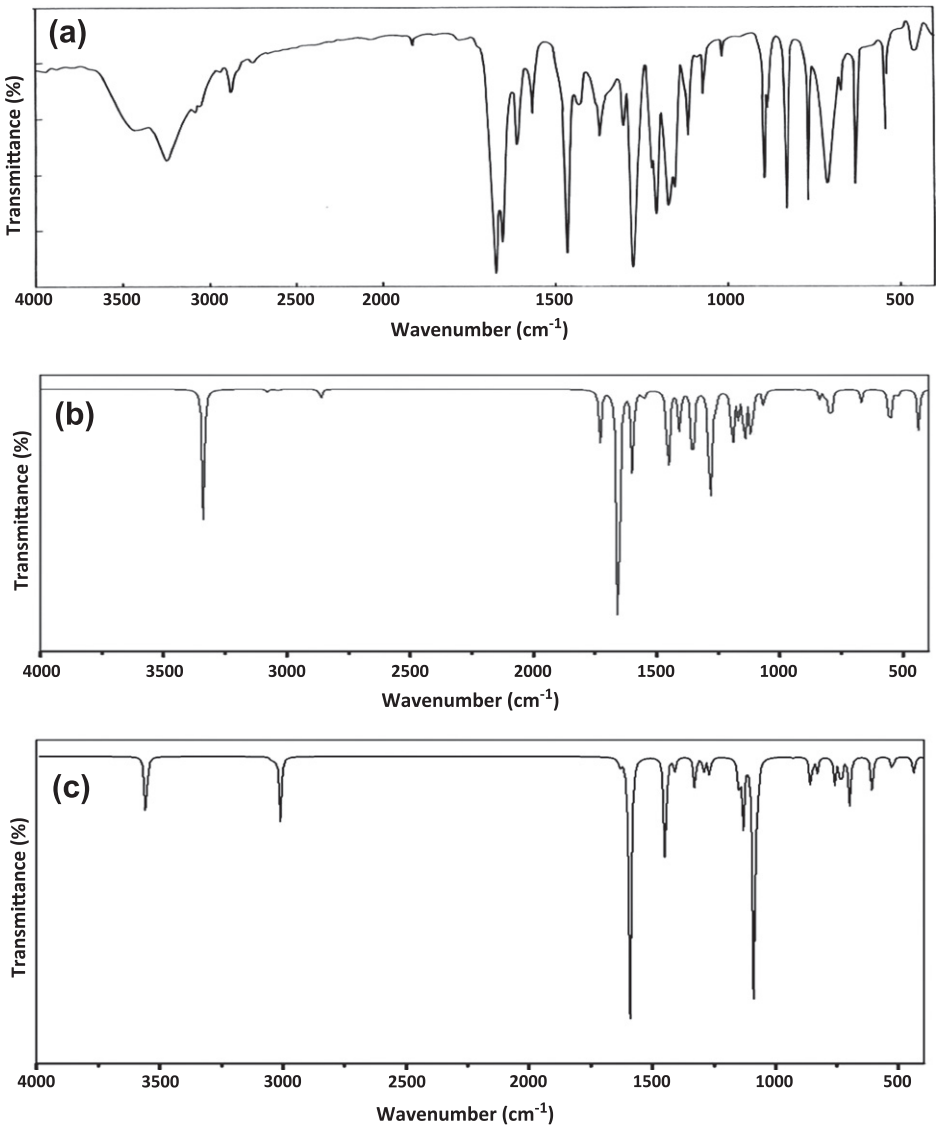

Fig. 3. Observed and calculated FT-IR spectra of 2-hydroxy-5-bromobenzaldehyde. (a) Observed (b) *cis* conformer (b) *transcis*-A conformer.

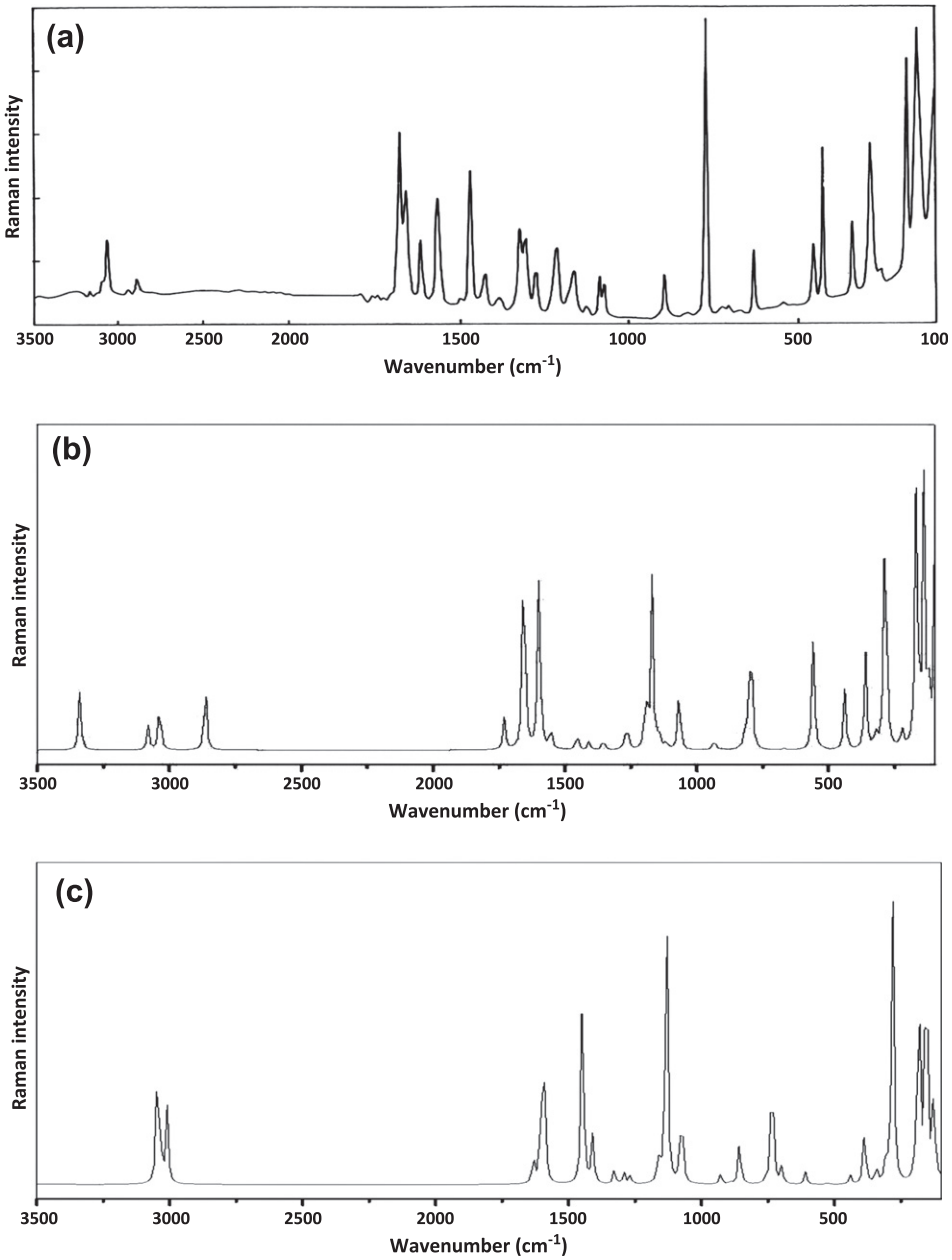

Fig. 4. Observed and calculated FT-Raman spectra of 2-hydroxy-5-bromobenzaldehyde. (a) Observed (b) *cis* conformer (b) *transcis*-A conformer.

with other vibrations. This is evident for the strong absorption at 1205 cm^{-1} in IR spectrum and medium absorption at 1207 cm^{-1} in Raman are compared to calculated wavenumbers of *cis* and *transcis-A* conformers at 1194, 1150 cm^{-1},respectively, are nearly correlated with experimental spectrum. The out-of-plane mode is assigned to a very strong shoulder at 428 cm^{-1} in Raman spectrum, which is observed in the calculated spectrum at 439 cm^{-1} in *cis* and 432 cm^{-1} in *transcis-A* conformers. It is a pure mode not mixed with any other modes. The B3LYP frequencies are in good agreement with both the in-plane and out-of-plane modes.

Generally, bands due to C—O stretching of the title molecule are of very strong intensities in both the IR and Raman spectra and appear around 1230–1270 cm^{-1}. Our calculations of C—O vibration modes on the basis level of 6-311G++(d,p) (1265 cm^{-1}) show a more satisfactory correspondence to experimental values (1273 cm^{-1} (IR), 1270 cm^{-1} (Raman)). The in-plane C—O bending vibration often occurs with sharp and strong intense band in Raman at 455 cm^{-1}. The scaled frequency at 122 and 127 cm^{-1} are assigned to C—O out-of-plane bending vibration of *cis* and *transcis-A* conformers, respectively.

5.4.2. Carbon–Carbon vibrations

The ring carbon–carbon stretching vibrations occur in the region 1430–1625 cm^{-1}. In general, the bands are of variable intensity and are observed at 1625–1590, 1575–1590, 1470–1540, 1430–1465 and 1280–1380 cm^{-1} from the frequency ranges given by Varsanyi [29] for the five bands in the region. In the present work, the frequencies observed in FT-IR spectrum at 1650, 1608, and 1461 cm^{-1} have been assigned to C—C stretching vibrations. The corresponding vibration appears in the FT-Raman spectrum at 1650, 1611, and 1458 cm^{-1}. The theoretically computed values of *cis* conformer at 1656, 1598, and 1454 cm^{-1} and the bands of *transcis-A* at 1603, 1590 cm^{-1} by B3LYP/6-311G++(d,p) method. These are shows excellent agreement with experimental data.

Table 5
The observed FT-IR, FT-Raman and calculated wave numbers (cm^{-1}) using B3LYP method with 6-311++G(d,p) basis set and probable assignments for cis and *transcis-A* conformers of 2-hydroxy-5-bromobenzaldehyde.

Symmetry species	Observed frequencies (cm^{-1})		Calculated frequencies (cm^{-1})				Vibrational assignments (>10% PED)
	FTIR	FT Raman	*cis*		*transcis-A*		
			Unscaled	Scaled	Unscaled	Scaled	
A″			98	96	72	71	τCHO(80)
A″			124	122	128	127	γCO(75)
A″			142	140	156	155	γC—Br(79)
A′		156vs	172	168	182	181	βC—CHO(64), βC—Br(11)
A″		183vs	227	223	193	192	γC—CHO(50)
A′		261vw	290	286	282	281	βC—Br(61)
A″		289vs	293	289	307	306	γCC(79)
A″		339vs	329	323	344	343	γCC(68)
A″			367	361	388	387	γCC(56)
A″		428vs	445	439	433	432	γOH(98)
A′		455s	532	524	442	441	βCO(27), νC—Br(14)
A′	551ms	549vw	562	554	527	526	νC—Br(48), βC=O(24), βCO(12)
A′			567	559	610	609	βC=O(61), βCC(26)
A′			570	562	689	688	βCC(30), νC—Br(18)
A′	631vs	627s	680	670	701	700	βCC(25), νC—Br(11)
A′	716vs	722vw	807	795	736	735	βCC(62), βC=O(21)
A″	767vs	766vs	827	815	762	761	γCH(77)
A″	829vs		852	840	832	831	γCH(76)
A′	898vs	894s	919	905	858	857	Ring breathing
A″			949	935	894	893	γCH of CHO(76)
A″	1074ms	1078s	1083	1067	922	928	γCH(77)
A′	1114ms	1115w	1132	1116	1076	1075	βCH(83)
A′	1148ms	1154s	1160	1144	1090	1089	βCH(30), νCC(22), νCO(11)
A′	1171vs	1174s	1186	1170	1133	1132	νC—CHO(21), νCC(16), βOH(12)
A′	1205vs	1207ms	1210	1194	1151	1150	βOH(38), νCC(21), νC—CHO(14)
A′	1273vs	1270vs	1283	1265	1164	1163	νCO(40), νC—CHO(29)
A′	1296ms	1301vs	1302	1284	1269	1268	βCH(41), νCC(27)
A′	1369s	1372vw	1375	1355	1293	1292	βCH of CHO(62)
A′	1421w	1417s	1428	1408	1329	1328	νCC(67)
A′	1461vs	1458vs	1474	1454	1410	1409	νCC(55), βOH(21)
A′	1568s	1564vs	1576	1554	1449	1448	νCC(24), βCH (13), βOH(11)
A′	1608s	1611s	1620	1598	1501	1500	νCC(52)
A′	1650s	1650vs	1680	1656	1604	1603	νCC(64)
A′	1674vs	1672vs	1754	1730	1634	1633	νC=O(86)
A′	2864s	2869w	2977	2863	3277	3010	νCH of CHO(99)
A′	2909vw	2913vw	3157	3036	3304	3035	νCH(99)
A′	3068vw	3065vs	3202	3080	3312	3042	νCH(100)
A′	3139vs		3273	3147	3319	3049	νCH(95)
A′	3366ms	3363ms	3472	3339	3872	3557	νOH(100)

vs: very strong; s: strong; ms: medium strong; w: weak; vw: very weak; *ν*: stretching; *β*: in-plane-bending; *γ*: out-of-plane bending; *τ*: twisting; PED: potential energy distribution.

The C—C aromatic stretch, known as semicircle stretching, predicted at 1554 cm^{-1} is in reasonable agreement with the band observed at 1568 cm^{-1} in FT-IR and at 1564 cm^{-1} in FT-Raman spectra. The medium strong band at 1421 cm^{-1} is observed in the FT-IR and the corresponding Raman band at 1417 cm^{-1} has a weak intensity. These bands arise from the scaled wavenumber at 1408 cm^{-1} in *cis* conformer, which can be described as C—C stretching mode [30].

The frequencies observed in FT-IR spectrum at 898 cm^{-1} have been assigned to ring breathing and corresponding vibration appear in FT-Raman spectrum at 894 cm^{-1}. The theoretically computed value of 905 cm^{-1} shows agreement with experimental observations. The in-plane deformation vibration is at higher frequencies than the out-of-plane vibrations. These are observed at 716, 631 cm^{-1} (IR), and 722, 627, 339, 289 cm^{-1} (Raman) are assigned to CCC deformation of phenyl ring. The theoretically computed values at 795, 670, 562, 361, 323, 289 cm^{-1} by B3LYP/6-311G++(d,p) method gives excellent agreement with experimental data.

5.4.3. C—H vibrations

Usually the bands around 3100–2900 cm^{-1} are assigned to C—H stretching vibration in aromatic compound. They are not appreciably affected by the nature of the substituents. In the present work, the bands 3139, 3068 and 2909 cm^{-1} are assigned to C—H stretching vibrations in FT-IR and the corresponding FT-Raman wavenumbers are ascribed to 3065 and 2913 cm^{-1}. The substitution sensitive C—H in-plane bending vibrations are assigned to the three very strong bands at 1301, 1154, 1115 cm^{-1} in FT-Raman and very strong bands at 1296, 1148, 1114 cm^{-1} in IR. The weak to strong IR bands observed at 1074, 829, 767 cm^{-1} and Raman bands at 1078, 766 cm^{-1} are assigned to C—H out-of-plane bending vibration. They are good agreement with literature value [31,32]. The B3LYP/6-311++G(d,p) calculated wavenumbers at 1284, 1144, 1116, 1067, 840, and 815 cm^{-1} are correlate with the experimental values.

5.4.4. C—CHO vibrations

In general, the C—CHO stretching vibration for aldehyde gives rise to band in the range 1230–1160 cm^{-1} [33]. The recorded spectrum show very strong intensity band at 1171 cm^{-1} in FT-IR and the strong intensity band obtained at 1174 cm^{-1} is at nearly the same frequency in Raman are attributed to C—CHO stretching vibration. In the present work the very strong intense band is obtained at 156 cm^{-1} in FT-Raman are assigned to the in-plane vibration of C—CHO. The out-of-plane bending vibration is attributed to

183 cm^{-1} in FT-Raman spectrum is present strongly. It may be noted that the frequency of the C—CHO out-of-plane bending vibration is higher that of the C—CHO in-plane bending vibration: the same effect is observed in similar systems [21,34].

5.4.5. —CHO vibrations

The aldehyde C—H and C=O stretching modes are easily assigned in substituted benzaldehyde, on account of their characteristics magnitudes. A very strong band observed at 1674 cm^{-1} in FT-IR and the same intense band observed at 1672 cm^{-1} in FT-Raman have been assigned to C=O stretching in the most important group wavenumber for aldehyde. Band due to C=O stretching, the force constant, and IR intensities are maximum at 17.584 m dyne $Å^{-1}$, and 279.936 kM mol^{-1}, respectively. These are presented in Table 6. The aldehydic C—H stretching wavenumber occurs lower than the most other C—H stretching vibrations. Two characteristic bands are usually observed due to the stretching vibration of the aldehydic C—H, both of which are the other in the region 2745–2650 cm^{-1} [35]. The presence of band at about 2864(IR) cm^{-1}, and 2869 cm^{-1} (Raman) are assigned to C—H stretching in aldehyde and a band due to the carbonyl stretching vibration in the region 1765–1685 cm^{-1} may usually be taken as indicating the presence of an aldehyde. A calculated band of *cis* conformer at 96 cm^{-1} assigned to a torsional vibration mode of C=O group. Thus, it may be conclude that a change in restoring force for C=O bond oscillator.

Table 6
The calculated IR intensities (kM mol^{-1}), and Raman intensity (Å amu^{-1}), using B3LYP/6-311++G(d,p) of cis and *transcis-A* conformers for 2-hydroxy-5-bromobenzaldehyde.

IR intensity		Raman intensity	
cis	*transcis-A*	*cis*	*transcis-A*
0.567	112.227	100	51.0772
4.148	0.9868	20.054	33.280
2.872	1.8963	88.909	99.061
24.105	1.2692	99.064	49.233
0.989	1.5892	7.445	20.744
2.264	1.2955	93.841	102.507
87.248	3.8805	6.981	10.008
5.868	2.5478	5.910	5.492
4.636	5.7890	33.665	21.501
5.596	2.005	1.1557	0.011
35.378	14.4684	20.121	3.079
7.675	15.7532	0.79132	0.720
37.169	31.3936	4.535	4.385
8.618	2.1987	31.182	0.550
0.051	42.9074	5.420	5.466
37.871	36.3766	0.5632	48.837
13.897	25.3255	51.390	0.9967
12.719	14.6505	9.648	0.182
8.518	34.2303	0.4764	17.523
2.261	0.1137	0.4068	0.863
0.849	1.0612	4.2363	3.814
5.282	38.1488	22.501	31.437
137.051	221.3092	2.7132	0.353
30.319	71.3977	6.591	97.832
87.642	23.3443	58.031	0.848
42.688	0.3204	21.191	9.262
114.272	17.9461	10.532	3.014
46.492	14.6816	1.0818	4.321
90.922	31.9851	4.230	5.056
64.325	12.4077	3.173	17.108
102.096	104.1550	6.0798	67.349
5.272	232.7833	8.385	30.6304
79.400	16.1135	65.529	31.978
279.936	9.8581	82.140	9.176
62.115	58.1318	10.718	25.871
11.464	4.2179	24.55	12.648
0.450	0.2816	18.335	10.806
4.870	1.7291	8.335	28.035
92.915	65.7467	20.342	17.875

The C—H stretching band although weak, is useful for characterization purposes. However, the overtone of the C—H in-plane deformations may disturb the position of the C—H stretching band or result in some confusion. The presence of two bands in the region 2915–2875 cm^{-1} is due to an interaction between the C—H stretching vibration and the overtone of C—H bending vibrations at 1369 (IR), 1372 (Raman) cm^{-1}. This involves Fermi resonance since aldehydes for which the latter band is shifted have only one band, this being in the region 2895–2805 cm^{-1}. Thus, the weak and very weak intensity band at around 2864 cm^{-1} is attributed to the aldehydic C—H stretching mode. The calculated band at 935 cm^{-1} is ascribed to the aldehydic deformation mode for cis conformer. The recorded spectrum does not show any such kind of bands in this region.

5.4.6. C—Br vibrations

Bromine compounds absorb strongly in the region 650–485 cm^{-1} due to C—Br stretching vibrations [33]. A weak band observed at 549 cm^{-1} in Raman and the medium strong band at 551 cm^{-1} in IR are assigned to the C—Br stretching vibration. The calculated wavenumber at 554 cm^{-1} of global minimum energy conformer show good agreement with the experimental wavenumber. A very weak Raman band at 261 cm^{-1} is assigned to the C—Br in-plane bending vibration, it is observed theoretically at 286 cm^{-1}. The C—Br out-of-plane bending vibration is obtained theoretically at 140 cm^{-1}.

5.5. Molecular orbital studies

The most widely used theory by chemists is the molecular orbital (MO) theory. It is important that Ionization Potential (IP), Electron Affinity (EA), Electrophilicity Index (ω), Chemical Potential (μ), Electronegativity (χ), Hardness (η), and First Excitation Energy (τ) be put into a MO framework. These are readily be done within the limitations of Koopman's theorem, the orbital energies of the frontier orbital is given by Fig. 5 show an orbital energy diagram for HBB molecule of *cis* and *transcis-A* conformers. Only the HOMO and LUMO orbitals are shown. We focus on the HOMO and LUMO energies in order to determine interesting molecular/atomic properties and chemical quantities. In simple molecular orbital theory approaches, the HOMO energy (ε_{HOMO}) is related to the IP by Koopmann's theorem and the LUMO energy (ε_{LUMO}) has been used to estimate the electron affinity (EA) [36]. If $-\varepsilon_{HOMO} \approx$ IP and $-\varepsilon_{LUMO} \approx$ EA, then the average value of the HOMO and LUMO energies is related to the electronegativity (χ) defined by Mulliken [37] with χ = (IP + EA)/2. In addition, the HOMO–LUMO gap is related to the hardness (η) [38–40], and also Parr et al. [41] defined global electrophilicity as a quantitative intrinsic numerical value and suggested the term electrophilicity index (ω), a new global reactivity descriptor of molecule, as $\omega = \frac{\mu^2}{2\eta}$ where μ is the chemical potential takes the average value [42] i.e., μ = –(IP + EA)/2. In general, the electrophiles are electron lovers or electron deficient and hence prefer to accept electrons and form bonds with nucleophiles. Thus electrophilicity is a useful structural depictor of reactivity and is frequently used in the analysis of the chemical reactivity of molecule [43]. The title molecule with low potential is a good electrophile, an extremely hard molecule has feeble electron acceptability. Consequently, a measure of molecular electrophilicity depends on both the chemical potential and the chemical hardness. Finally, the calculated HOMO–LUMO gaps are also closer to the first electronic excitation energies (τ). The electronegativity and hardness are of course used extensively to make predictions about chemical behavior and these are used to explain aromaticity in organic compounds [44]. Fig. 5 offer a concise and graphic definition of chemical hardness. A hard molecule has a large HOMO–LUMO gap and a soft molecule has a small HOMO–LUMO

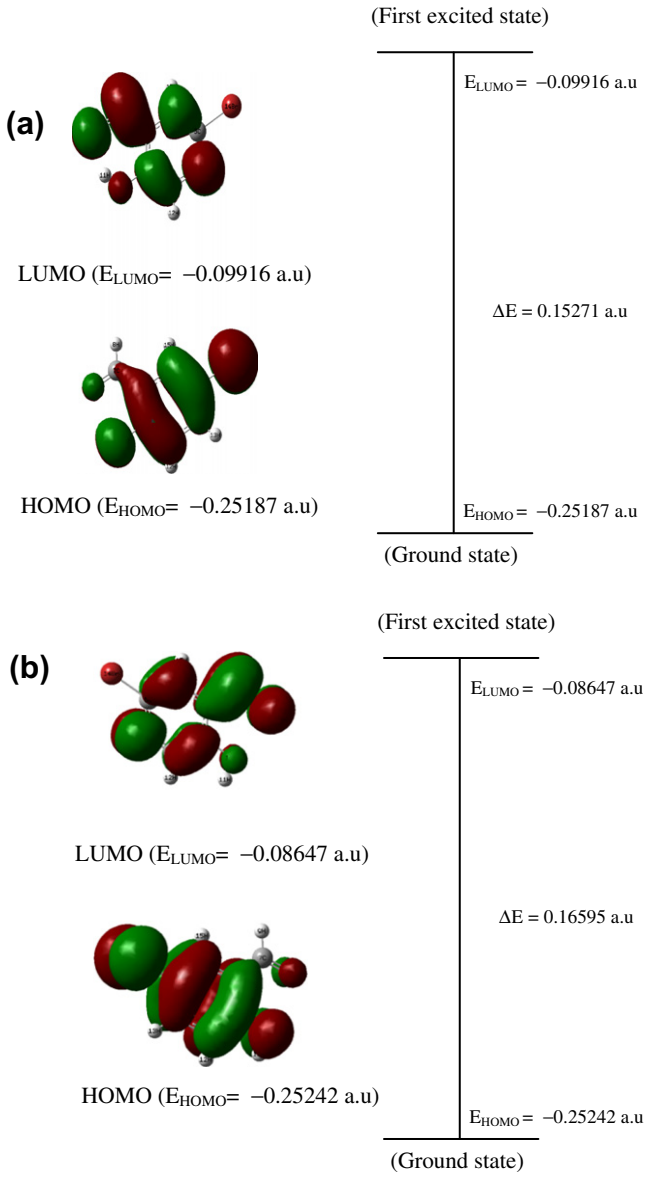

Fig. 5. The atomic orbital compositions of the frontier molecular orbital for (a) *cis* and (b) *transcis-A* conformers of HBB.

gap. In quantum theory, changes in the electron density of a chemical system result from the mixing of suitable excited-state wave function with the ground-state wave function. The mixing coefficient is inversely proportional to the excitation energy between the ground and excited state. A small HOMO–LUMO gap automatically means small excitation energies to the manifold of excited states. Therefore, soft molecule, with a small gap, will have their electron density changed more easily than a hard molecule.

In terms of chemical reactivity, we can conclude that soft molecule will be more reactive than hard molecule. When I is small and A is large and positive the molecule should be soft. If we had the exact electron density for the system, we would have the exact orbital energy and chemical potential, which would be constant everywhere. For an approximate density, μ would not be constant everywhere. Electron density would move from regions where μ was too positive to regions where μ was too negative, until equilibrium was reached and the energy minimized.

On the basis of a fully optimized ground state structure, the DFT/B3LYP/6-311++G(d,p) calculation predicts one intense

Table 7
Calculated physico-chemical properties for title molecule of cis and *transcis-A* conformers correlated with molecular orbital theory at B3LYP method.

Parameters	*cis*	*transcis-A*
HOMO energy ($-\varepsilon_{HOMO}$)	−0.25187 a.u.	−0.25242
LUMO energy ($-\varepsilon_{LUMO}$)	−0.09916 a.u.	−0.08647
HOMO–LUMO energy gap in eV	−0.15271 a.u.	−0.16595
Ionization potential (IP)	−0.25187 a.u.	−0.25187
Electron affinity (EA)	−0.09916 a.u.	−0.08647
Electrophilicity index (ω)	0.100857	0.08650
Chemical potential (μ)	0.17551	0.169445
Electronegativity (χ)	−0.17551	−0.169445
Hardness (η)	−0.15271 a.u.	−0.16595
First excitation energy (τ)	0.15271	−0.08647

electronic transition from the ground to the first excited state and is mainly described by one electron excitation from the highest occupied molecular orbital (HOMO) to the lowest unoccupied molecular orbital (LUMO).

The HOMO is located over Br atom and OH group, and the HOMO → LUMO transition implies an electron density transfer to the aldehydic group. Moreover, these orbital significantly overlap in their position for HBB. The atomic orbital compositions of the frontier molecular orbital are sketched in Fig. 5. The HOMO–LUMO energy gap of *cis* and *transcis-A* conformers for HBB were calculated at the B3LYP/6-311++G(d,p) level, which reveals that the energy gap reflects the chemical activity of the molecule. The LUMO as an electron acceptor represents the ability to obtain an electron and HOMO represents the ability to donate an electron. The energy gap between the HOMO and the LUMO molecular orbitals is a critical parameter in determining molecular electrical transport properties because it is a measure of electron conductivity. The energy values of HOMO are computed −0.25187, and −0.25242 a.u. and LUMO are −0.09916, −0.08647 a.u. and the energy gap values are −0.15271, −0.16595 a.u. in *cis* and *transcis-A* conformers of HBB, respectively. Lower value in the HOMO and LUMO energy gap explains the eventual charge transfer interactions taking place within the molecule. The calculated chemical hardness (η), chemical potential (μ), electrophilicity values (ω), ionization potential (IP), electron affinity (EA), electronegativity (χ), first electron excitation (τ) are presented in Table 7.

5.6. Molecular electrostatic potential maps

The molecular electrostatic potential (MESP) mapping is very useful in the investigation of the molecular structure with its physiochemical property relationship [45–49]. The molecular electrostatic potential surface (MESP) which is a stratagem of electrostatic potential mapping onto the iso-electron density surface simultaneously displays molecular shape, size and electrostatic potential values and it has been plotted for molecule under investigation using B3LYP method. The MESP map of 2-hydroxy-5-bromobenzaldehyde visibly suggests that the region around carbon atoms linked through oxygen atoms O9, O10 in aldehyde and hydroxyl groups represents the most negative potential region (red[1]). The hydrogen atoms attached to the ring beat the maximum bang of positive charge (blue). The color scheme for the MESP surface is red, electron rich, partially negative charge; blue, slightly electron deficient, partially positive charge; light blue, slightly electron deficient region; yellow, slightly electron rich region, respectively. The MESP total density of title molecule clearly shows the presence of more electron density around the aldehyde and hydroxyl groups characterized by red color. The predominance of green region

[1] For interpretation of color in Fig. 6, the reader is referred to the web version of this article.

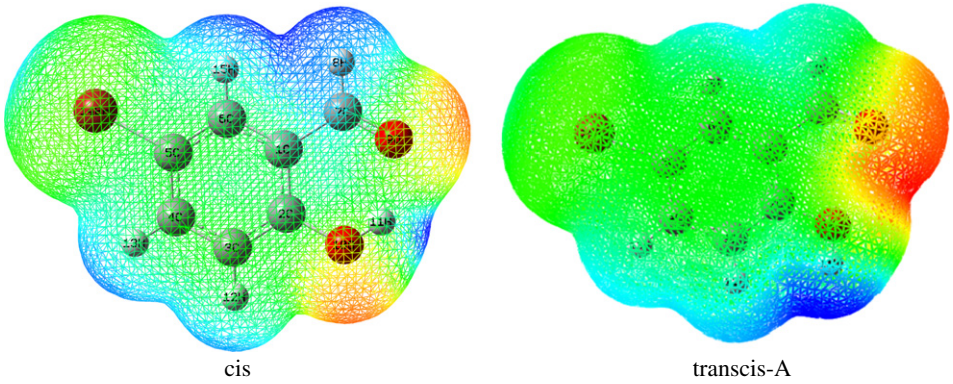

Fig. 6. Calculated 3D molecular electrostatic potential contour map of *cis* and *transcis-A* conformers of HBB. The electron density isosurface is 0.02 a.u.

in the MESP surfaces corresponds to a potential halfway between the two extremes red and dark blue color. The MESP and total density plots for most negative potential (−0.1843 eV) and most positive potential (2.1562 eV) for B3LYP/6-311++G(d,p) method is given in Fig. 6. (For interpretation of the references to color in this paragraph, the reader is referred to the web version of the article). On the other hand, the red region was not seen clearly in the oxygen atom of hydroxyl group, moreover it is concentrated on aldehydic oxygen atom of *transcis-A* conformer. The results suggest that the *cis* conformer found to be useful to both bond metallically and interact intermolecularly. This result was also supported by the evidences of charge analyses part.

5.7. Hyperpolarizability calculations

The polarizability α and the hyper polarizability β and the electric dipole moment μ of the HBB are calculated by finite field method using B3LYP/6-311++G(d,p) basis set available in DFT package. To calculate all the electric dipole moments and the first hyperpolarizabilities for the isolated molecule, the origin of the Cartesian coordinate system $(x, y, z) = (0, 0, 0)$ was chosen at own center of mass of HBB.

The first hyperpolarizability (β_0) of this noval molecular system and related properties (β, α_0 and $\Delta\alpha$) of HBB are calculated and it is based on the finite-field approach. In the presence of an applied electric field, the energy of a system is a function of the electric field. First hyperpolarizability is a third rank tensor that can be described by a $3 \times 3 \times 3$ matrix. The 27 components of the 3D matrix can be reduced to 10 components due to the Kleinman symmetry [50]. It can be given in the lower tetrahedral format. It is obvious that the lower part of the $3 \times 3 \times 3$ matrixes is a tetrahedral. The components of β are defined as the coefficients in the Taylor series expansion of the energy in the external electric field. When the external electric field is weak and homogeneous, this expansion becomes:

$$E = E^0 - \mu_\alpha F_\alpha - 1/2\alpha_{\alpha\beta}F_\alpha F_\beta - 1/6\beta_{\alpha\beta\gamma}F_\alpha F_\beta F_\gamma + \cdots$$

Where E^0 is the energy of the unperturbed molecules, F_α is the field at the origin μ_α, $\alpha_{\alpha\beta}$ and $\beta_{\alpha\beta\gamma}$ are the components of dipole moment, polarizability and the first hyperpolarizability, respectively. The total static dipole moment μ, the mean polarizability α_0, the anisotropy of the polarizability $\Delta\alpha$ and the mean first hyperpolarizability β_0, using the x, y, z components they are defined as:

$$\mu = (\mu_x^2 + \mu_y^2 + \mu_z^2)^{1/2}$$

$$\alpha_0 = \frac{\alpha_{xx} + \alpha_{yy} + \alpha_{zz}}{3}$$

$$\alpha = 2^{-1/2}[(\alpha_{xx} - \alpha_{yy})^2 + (\alpha_{yy} - \alpha_{zz})^2 + (\alpha_{zz} - \alpha_{xx})^2 + 6\alpha_{xx}^2]^{1/2}$$

$$\beta_0 = (\beta_x^2 + \beta_y^2 + \beta_z^2)^{1/2}$$

$$\beta_x = \beta_{xxx} + \beta_{xyy} + \beta_{xzz}$$

$$\beta_y = \beta_{yyy} + \beta_{xxy} + \beta_{yzz}$$

$$\beta_z = \beta_{zzz} + \beta_{xxz} + \beta_{yyz}$$

The DFT/6-311++G(d,p) calculated first hyperpolarizability of HBB is 12.67×10^{-30} esu, and is shown in Table 8. The calculated values of μ_{tot}, α_{tot}, and β_{tot} for the title compound are 5.288 D, 46.73×10^{-24} esu and 12.67×10^{-30} esu, which are greater than those of urea (the μ_{tot}, α_{tot}, and β_{tot} of urea are 1.373 D, 3.8312×10^{-24} esu and 0.37289×10^{-30} esu obtained by B3LYP/6-31G(d) method [51]. Theoretically, the first-order hyperpolarizability of the *cis* conformer of molecule is of 33.98 times magnitude of urea. However, *transcis-A* conformer is of 47.78 times magnitude of urea. These results indicate that the *cis* and *transcis-A* conformers of title molecule are good candidate of NLO material. As can be seen from the β_{tot} value for this molecule, the larger value of first hyperpolarizability corresponds to the lower HOMO–LUMO gap. This correlation is reported in the literature [52].

Table 8
The electric dipole moment μ (D) the average polarizability α_{tot} ($\times 10^{-24}$ esu) and the first hyperpolarizability β_{tot} ($\times 10^{-30}$ esu) of cis and *transcis-A* conformers for HBB.

Parameters	cis	*transcis-A*
μ_x	2.5169	−2.0806
μ_y	−4.6514	2.1967
μ_z	0.00	0.2856
μ	5.288	3.0390
α_{xx}	−62.141	−88.6776
α_{xy}	−9.5887	8.2456
α_{yy}	−75.9854	−56.8675
α_{xz}	0.00	0.0647
α_{yz}	0.00	0.0249
α_{zz}	−72.3993	−72.6858
$\langle\alpha\rangle$	124.242	155.912
α_{tot} (esu)	46.73×10^{-24}	72.7436×10^{-24}
β_{xxx}	−30.2384	−150.2990
β_{xxy}	−27.4157	36.8838
β_{xyy}	−21.0905	−2.4712
β_{yyy}	−76.0074	9.6065
β_{xxz}	0.00	1.5155
β_{xyz}	0.00	−0.0322
β_{yyz}	0.00	0.6173
β_{xzz}	−21.4369	−20.4416
β_{yzz}	−0.2987	−4.8325
β_{zzz}	0.00	0.6649
β_{tot} (esu)	12.67×10^{-30}	17.817×10^{-30}

Table 9
Thermodynamic properties at different temperatures at the B3LYP/6-311G++(d,p) level for cis conformer of 2-hydroxy-5-bromobenzaldehyde.

T (K)	$C^0_{p,m}$ (cal mol^{-1} K^{-1})	S^0_m (cal mol^{-1} K^{-1})	ΔH^0_m (kcal mol^{-1})
200	7.2249	19.4566	12.2317
300	17.3691	43.2933	25.9302
400	31.9850	75.9178	43.9968
500	51.3267	117.9104	66.5837
600	74.9933	167.7520	92.7587
700	102.9527	223.2562	121.8694

5.8. Thermodynamic properties

The total energy of a molecule is the sum of translational, rotational, vibrational and electronic energies, i.e., $E = E_t + E_r + E_v + E_e$. The statistical thermo chemical analysis of HBB is carried out considering the molecule to be at room temperature of 298.15 K and one atmospheric pressure. The thermodynamic parameters, like rotational constant, zero point vibrational energy (ZPVE) of the molecule by DFT method with B3LYP are presented in Table 3 for C1 conformer. On the basis of vibrational analysis and statistical thermodynamics, the standard thermodynamic functions: heat capacity ($C^0_{p,m}$), entropy (S^0_m), and enthalpy (H^0_m) were obtained and listed in Table 9. As is evident from Table 9, all the values of $C^0_{p,m}$, S^0_m, and H^0_m increases with the increase of temperature from 100.0 K to700.0 K, which is attributed to the enhancement of the molecular vibration while the temperature increases because at a constant pressure (db = 1 atm) values of $C^0_{p,m}$, S^0_m, and H^0_m are equal to the quantity of temperature [53]. The correlations between these thermodynamic properties and temperatures T are fitted by quadratic formulas as follows and corresponding fitting factors (R^2) for these thermodynamic properties are found to be 1, 0.999 and 0.999 for heat capacity, entropy, and enthalpy, respectively. The temperature dependence correlation graphs are shown in Figs. 7–9. Notice: all the thermodynamic calculations were done in gas phase and they could not be used in solution. Scale factors have been recommended [54] for an accurate prediction in determining the zero-point vibration energies, heat capacities, entropies, enthalpies.

$$C^0_{p,m} = 0.166 + 0.009T + 0.000T^2 \times 10^{-4}; \quad (R^2 = 1)$$

$$S^0_m = -6.161 + 0.044T + 0.000T^2 \times 10^{-4}; \quad (R^2 = 0.999)$$

$$H^0_m = -4.709 + 0.044T + 0.000T^2 \times 10^{-4}; \quad (R^2 = 0.999)$$

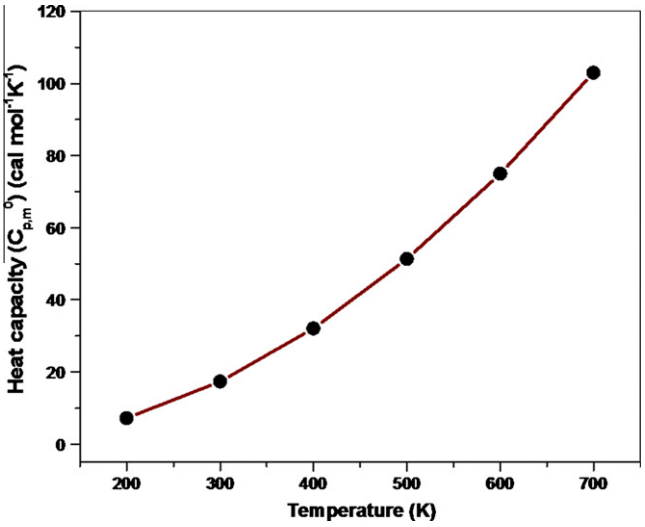

Fig. 7. Correlation graph of heat capacity and temperature for HBB.

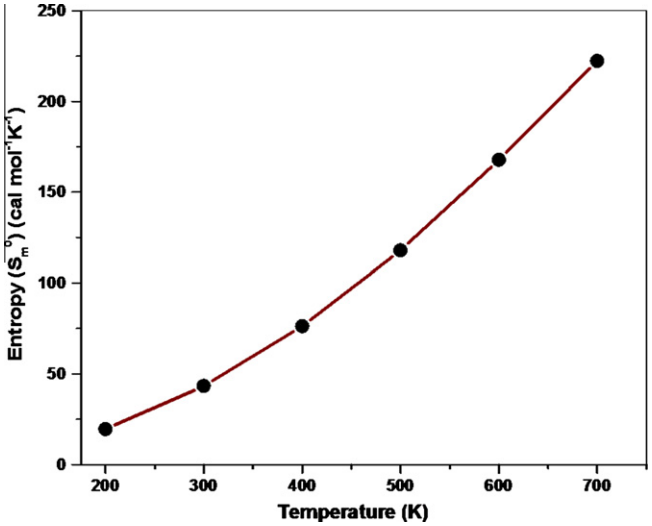

Fig. 8. Correlation graph of entropy and temperature for HBB.

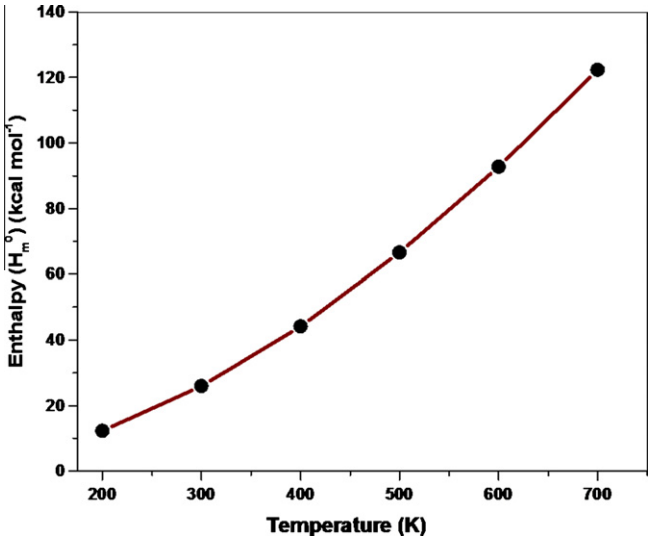

Fig. 9. Correlation graph of enthalpy and temperature for HBB.

All these thermodynamic data provide helpful information for further study on HBB. They can be used to compute the other thermodynamic parameters according to relationships of thermodynamic functions and to determine the directions of chemical reactions according to the second law of thermodynamics [55].

Dipole moment reflects the molecular charge distribution and is given as a vector in three dimensions. Therefore, it can be used an illustrator to depict the charge movement across the molecule. Direction of the dipole moment vector in a molecule depends on the centers of negative and positive charges. Dipole moments are strictly identified for neutral molecules. For charged systems, its value depends on the choice of origin and molecular orientation. As a result the dipole moment of title molecule was observed as 5.288 D with B3LYP/6-311++G(d,p) method [56].

6. Conclusion

The FT-IR and FT-Raman spectral studies of 2-hydroxy-5-bromobenzaldehyde were carried out for the first time. A complete vibrational and molecular structure analysis has been performed based on the quantum mechanical approach by DFT calculation.

The equilibrium geometries and harmonic frequencies were determined and analyzed for the most stable conformer *cis* and other nearest energy conformer *transcis-A* using DFT level with 6-311G++(d,p) basis set. The difference between the observed and scaled wavenumber values of the most of the fundamental is very small. Therefore the assignments with reasonable deviation from the experimental value seem to be correct. This study demonstrates that scaled DFT (B3LYP) calculations are powerful approach for understanding the vibrational spectra of the title molecule. NBO results reflects the charge transfer mainly due to C=O group. The calculated HOMO and LUMO energy gap (−0.15271, −0.16595 a.u.) are confirm the presence of charge transfer within the *cis* and *transcis-A* conformers of the molecule. The calculated HOMO and LUMO energies can be used to semiquantitatively estimate the ionization potential, electron affinity, electronegativity, electrophilicity index, hardness, chemical potential and first electron excitation energy. The predicted MESP contour map shows the negative regions at aldehydic oxygen, it is subjected to the electrophilic attack of the *cis* conformer. The theoretically constructed FT-IR and FT-Raman spectra shows good correlation with experimentally observed FT-IR and FT-Raman spectra. Thermodynamic properties in the range from 100 K to 700 K are obtained. The gradients of $C_{p,m}$, S_m, H_m, and vibrational intensity increases with increase of temperature.

References

[1] E.-R. Kenawy, F. Imam Abdel-hay, A. Abou el-Magd, Y. Mahmoud, J. Bioactive Compatible Polym. 20 (2005) 95.
[2] orgchem.colorado.edu/courses/3381manualS07/AldolLMchalcones81S07.
[3] N. Karger, A.M. Amrin da costa, P.J.A. Ribeiro-Claro, J. Phys. Chem. A 103 (1999) 8672.
[4] J.H.S. Green, D.J. Harrison, Spectrochim. Acta 32A (1976) 1265.
[5] H. Lampert, W. Mikenda, A. Karpfen, J. Phys. Chem. A 101 (1997) 2254.
[6] R.A. Yadav, I.S. Singh, Ind. J. Phys. 58 13 (6) (1984) 556.
[7] S. Pinchas, Anal. Chem. 29 (3) (1957) 334.
[8] D.N. Singh, L.D. Singh, R.A. Yadav, Ind. J. Phys. 76 B (1) (2002) 35.
[9] P.J.A. Ribeiro-Claro, M.G.B. Drew, V. Felix, Chem. Phys. Lett. 356 (2002) 318.
[10] A. Nataraj, V. Balachandran, T. Karthick, J. Mol. Struct. 1006 (2011) 104–112.
[11] P. Bednarek, T. Bally, J. Gebicki, J. Org. Chem. 67 (2002) 1319.
[12] G. Chung, O. Kwon, Y. Kwon, J. Phys. Chem. A 102 (1998) 2381.
[13] P.J.A. Ribeiro-Claro, L.A.E. Batista de Carvalho, A.M. Amado, J. Raman Spectrosc. 28 (1997) 867.
[14] M.J. Frisch, G.W. Trucks, et al., GAUSSIAN 09, Revision A. 02, Gaussian, Inc., Wallingford, CT, 2009.
[15] G. Keresztury, S. Holly, J. Varga, G. Besenyei, A.Y. Wang, J.R. Durig, Spectrochim. Acta 49A (1993) 2007.
[16] G. Keresztury, J.M. Chalmers, P.R. Griffith (Eds.), Raman Spectroscopy, vol. 1, John Wiley & Sons Ltd., New York, 2002.
[17] Mehmet Karabacak, Mehmet Cinar, Sahin Ermec, Mustafa Kurt, J. Raman Spectrosc. 41 (2010) 98.
[18] H.B. Schlegel, J. Comput. Chem. 3 (1982) 214.
[19] N. Sundaraganesan, S. Illakiamani, H. Saleem, P.M. Wojciechowski, D. Michalska, Spectrochim. Acta 61A (2005) 2995.
[20] T. Sundius, MOLVIB: Quantum Chemistry Programme Exchange Programme No. 807, 1991.
[21] H. Mollendal, S. Gundersen, M.A. Tafipolsky, H.V. Volden, J. Mol. Struct. 444 (1998) 47.
[22] M. Szafran, A. Komasa, E.B. Adamska, J. Mol. Struct. (Theochem.) 827 (2007) 101.
[23] C. James, A. Amal Raj, R. Rehunathan, I. Hubert Joe, V.S. Jayakumar, J. Raman Spectrosc. 37 (2006) 1381.
[24] Liu Jun-na, Chen Zhi-rang, Yuan Shen-fang, J. Zhejiag, University Sci. 6B (2005) 584.
[25] S. Sebastian, N. Sundaraganesan, Spectrochim. Acta 75A (2010) 941.
[26] S. Bratoz, D. Hadzi, N. Sheppard, Spectrochim. Acta 8A (1956) 249.
[27] A. Ramoji, J. Yenagi, J. Tonannavar, Spectrochim. Acta 69A (2008) 926.
[28] G. Socrates, Infrared Characteristic Group Frequencies, John Wiley, GB, 1980.
[29] G. Varsanyi, Vibrational Spectra of Benzene Derivatives, Akademiai Kiado, Budapest, 1969.
[30] F.R. Dollish, W.G. Fateley, F.F. Bantley, Characteristic Raman Frequencies of Organic Compounds, Wiley, New York, 1974. 170.
[31] V. Krishnakumar, V. Balachandran, Spectrochim. Acta 63 A (2006) 464.
[32] S. Mohan, A.R. Prabhakaran, Asian J. Chem. 2 (1990) 196.
[33] G. Socrates, Infrared and Raman Characteristic Group Frequencies-Tables and Charts, third ed., Wiley, New York, 2001. p. 124.
[34] G.P. Kushto, P.W. Jagodzinski, Spectrochim. Acta 54A (1998) 799.
[35] E.L. Saier, L.R. Cousins, M.R. Basila, Anal. Chem. 34 (1962) 824.
[36] P. Politzer, F. Abu-Awwad, Theor. Chem. Acta 99 (1998) 83.
[37] R.S. Mulliken, J. Chem. Phys. 2 (1934) 782.
[38] R.G. Parr, R.G. Pearson, J. Am. Chem. Soc. 105 (1983) 7512.
[39] R.G. Parr, W. Yang, Density Functional Theory for Atoms and Molecules, Oxford University Press, New York, 1982.
[40] R.G. Pearson, Chemical hardness, John Wiley-VCH, Weinheim, 1997.
[41] R.G. Parr, L. von Szentpaly, S. Liu, J. Am. Chem. Soc. 121 (1999) 1922–1924.
[42] J. Padmanabhan, R. Parthasarathi, V. Subramanian, P.K. Chattaraj, J. Phys. Chem. A 111 (2007) 1358–1361.
[43] P.K. Chattaraj, B. Maiti, U. Sarkar, J. Phys. Chem. A 107 (2003) 4973–4975.
[44] F. De Proft, P. Geerlings, Chem. Rev. 101 (2001) 1451.
[45] P. Politzer, D.G. Truhlar (Eds.), Chemical Application of Atomic and Molecular Electrostatic Potentials, Plenum, New York, 1981.
[46] P. Politzer, K.C. Daiker, The Force Concept in Chemistry, Van Nostrand Reinhold Co., 1981.
[47] P. Politzer, P.R. Laurence, K. Jayasuriya, J. McKinney, Health Perspect. 61 (1985) 191.
[48] P. Politzer, J.S. Murray, in: D.L. Protein, R. Beveridge, Lavery (Eds.), Theoretical Biochemistry and Molecular Biophysics: A Comprehensives Survey, vol. 2, Adenine Press, Schenectady, NY, 1991.
[49] E. Scrocco, J. Tomasi, Topics in Current Chemistry, vol. 42, Springer-Verlag, Berlin, 1973. p. 95.
[50] D.A. Kleinman, Phys. Rev. 126 (1962) 1977.
[51] Y.X. Sun, Q.L. Hao, W.X. Wei, Z.X. Yu, L.D. Lu, X. Wang, Y.S. Wang, J. Mol. Struct.: THEOCHEM 904 (2009) 74.
[52] Hasan. Tanak, J. Mol. Struct.: THEOCHEM 950 (2010) 5–12.
[53] F. Bopp, J. Meixner, J. Kestin, Thermodynamics and Statistical Mechanics, fifth ed., Academic Press Inc. (London) Ltd., New York, 1967.
[54] G. Varsanyi, P. Sohar, Acta Chim. Acad. Sci. Hung. 74 (1972) 315–333.
[55] R. Zhang, B. Dub, G. Sun, Y. Sun, Spectrochim. Acta 75A (2010) 1115–1124.
[56] M. Suzuki, K. Kozima, Bull. Chem. Soc. 42 (1969) 2183–2186.